한국해양공학회지 제17권 제1호, pp 33~40, 2003 (ISSN 1225-0767)

Vibration Suppression of Moving Suspended Systems by Wave Absorption Control

MUNEHARU SAIGO* AND DONG-HO NAM**
*Smart Structure Research Center,
National Institute of Advanced Industrial Science and Technology (AIST), Tsukuba, Japan
**Dept. of Mechanical Design Engineering, Incheon City College, Incheon, Korea, Currently with AIST, Japan

KEY WORDS : Vibration Control, Wave Absorption Control, Multiple-pendulum, Wire-load System, Imaginary System

ABSTRACT : *기존 대부분의 진동제어법이 모드제어에 근거한 것인데 반면, 본 연구에서는 진동억제의 또다른 방법인 파동제어기법을 다루었다. 무반사조건을 만족하면서 진동에너지를 흡수하는 파동제어는 특히 1차원 구조계에 유용하게 사용될 수 있으리라고 기대되는데, 현실적으론 제어알고리즘의 실현화에 그 어려움이 있다. 본 연구에서는 근사화된 무한구조계를 계산기내에 구축하여, 진동에너지가 근사 무한구조계에 흡수되는 조건을 제어기가 실현하는 제어수법을 개발하였다. 시뮬레이션과 실험을 통하여, 본 연구에서 제안한 파동제어기법에 의해 이동하는 현수체의 진동억제가 효율적으로 이루어짐을 확인할 수가 있었다.*

1. Introduction

Recently, traveling-wave control has been studied as an alternative to mode-based vibration control by several researchers. Wave control has several advantages over mode-based vibration control; it has no control and observation spillovers that may occur in the vibration control when there are some imperfections in system modeling or inaccuracy in sensor locations; it has better control performance than vibration control at low frequencies; and it is basically a local control method to which we have paid attention in our studies. The last feature means that we can suppress the vibration of a system using no more than the information about the dynamic states of the element nearest the actuator. This is quite advantageous to the system whose parameters are changeable during control operations.

The studies of traveling-wave control include Vaughan(1968), Von Flotow (1986a, 1986b), Millar and Von Flotow(1989), Mace(1984), Fujii and Ohtsuka(1992), Tanaka (1992) and Utsumi(1999).

These studies of traveling-wave control of elastic beams or strings have used the theoretical solution expressed in the form of traveling wave and derived the non-reflecting condition of waves at the control point. On the other hand, O'connor and Lang(1998) treated a mass-and-spring system and presented a method of the wave-absorption in a discrete vibration system. In these studies, few attempts have been made to apply the wave control strategy to practical vibrating systems to show the above-mentioned advantages of traveling-wave control.

In the previous paper(Saigo et al., 1998), we presented a new practical wave control strategy that is easy to build in a control computer with on-line calculation of the imaginary wave-propagating system. We applied the presented method to the vibration suppression of a multiple-pendulum system and showed the effectiveness of the method experimentally. There, vibration control by controlling the support movement was addressed and no support movement for traveling toward a given target position was considered.

In the present paper, the wave control method presented in the previous paper is expanded to consider the combination of traveling control and vibration control. In this case, the control system has to achieve a system displacement to a desireds target position while suppressing the vibration. Both a multiple-pendulum system and a wire-and-load suspended system are treated. Furthermore, the method is applied to a model crane system and shown to be useful for the vibration suppressing of a practical crane.

2. Equation of Motion

2.1 Multiple-pendulum system

Fig. 1 shows a traveling multiple rigid-pendulum system and a traveling wire-and-load system. The equations of motion of a traveling multiple-pendulum system of n degrees of freedom(DOF) are obtained using the Lagrange's equation of motion. The kinetic energy T_k and the potential energy U_k of the k-th pendulum are expressed as

제1저자 M. Saigo 연락처: Tsukuba Central 2, Ibaraki, Japan
+81-29-861-7085 m.saigo@aist.go.jp

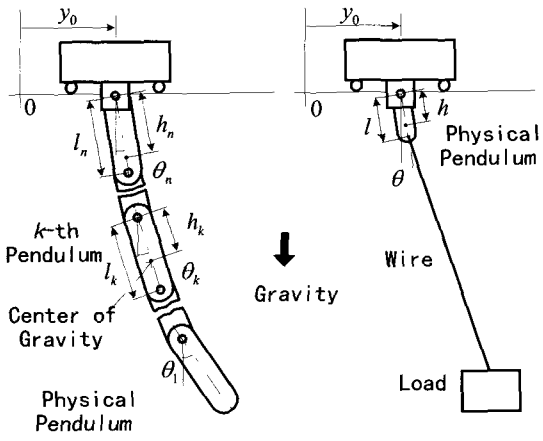

Fig. 1 Moving multiple-pendulum and wire-load system

$$U_k = -m_k g\left\{h_k(1-\theta_k^2/2) + \sum_{j=k+1}^{n} l_j(1-\theta_j^2/2)\right\}$$
$$T_k = m_k(\dot{y}_0 + \sum_{j=k+1}^{n} l_j\dot{\theta}_j)^2/2 + I_k\dot{\theta}_k^2/2 + m_k(\dot{y}_0 + \sum_{j=k+1}^{n} l_j\dot{\theta}_j)\dot{\theta}_k h_k \quad (1)$$

where θ_k is the angle of the k-th pendulum numbered from the free end and assumed to be so small that the terms having powers higher than second of θ_k are negligible, h_k is the distance between the center of gravity of the k-th pendulum and the axis of the k-th connecting pin, I_k is the moment of inertia of the k-th pendulum about the axis of the k-th connecting pin, m_k is the mass of k -th pendulum, l_k is the distance between the axes of the k-th and (k-1)-th connecting pins, and y_0 is the position of the support of the pendulum system.

The Lagrangian $L = \sum_{k=1}^{n}(T_k - U_k)$ gives the equations of motion of k-th pendulum as

$$(I_k + l_k^2\sum_{i=1}^{k-1} m_i)\ddot{\theta}_k + l_k\sum_{j=1}^{k-1}(l_j\sum_{i=1}^{j-1} m_i + h_j m_j)\ddot{\theta}_j + (l_k\sum_{i=1}^{k-1} m_i + h_k m_k)\sum_{i=k+1}^{n}(l_i\ddot{\theta}_i) + g(l_k\sum_{i=1}^{k-1} m_i + h_k m_k)\theta_k = 0 \quad (2)$$

From the equations obtained by replacing k by k+1 and by k-1 in Eq.(2), as well as Eq.(2) itself, the following equation is obtained.

$$-\{q_1 p_1 + J_1/(r_1 m_1)\}\ddot{\theta}_1 + q_2 p_1\ddot{\theta}_2 + g(m_1 + r_2 m_2)p_1(-\theta_1 + \theta_2) = 0$$
$$q_{k-1}p_{k-1}\ddot{\theta}_{k-1} - [q_k p_k + \{J_k + l_k(1-r_{k-1})m_{k-1}\}p_{k-1}]\ddot{\theta}_k + q_{k-1}p_k\ddot{\theta}_{k-1} + g\left\{\sum_{j=1}^{k-2} m_j + r_{k-1}m_{k-1})p_{k-1}\theta_{k-1} - (\sum_{j=1}^{k-1} m_j + r_k m_k)(p_k + p_{k-1})\theta_k + (\sum_{j=1}^{k} m_j + r_{k+1}m_{k+1})p_k\theta_{k+1}\right\} = 0 \qquad (k \neq 1, n)$$

$$q_{n-1}p_{n-1}\ddot{\theta}_{n-1} - \{J_n + l_n(1-r_{n-1})m_{n-1}\}p_{n-1}\ddot{\theta}_n + gp_{n-1}\left\{(\sum_{j=1}^{n-2} m_j + r_{n-1}m_{n-1})\theta_{n-1} - (\sum_{j=1}^{n-1} m_j + r_n m_n)\theta_n\right\} = -\ddot{y}_0$$
$$r_k = h_k/l_k\ ,\ J_k = I_k/l_k\ ,\quad p_k = 1/\{(1-r_k)m_k + r_{k+1}m_{k+1}\}\ ,\ q_k = J_k - h_k m_k \quad (3)$$

From the above equation, we see the term of the support movement appears explicitly only in the equation of the uppermost pendulum.

2.2 Wire-and-load system

The wire-and-load system shown in Fig.1 has a small rigid pendulum between the support and the wire, and there is a load at the bottom of the wire. The wire length is fixed. Assuming the equation of the wire is expressed by that of a dangling string and applying the finite difference method to the equation of motion, we obtain a system of equations similar to that of a multiple simple-pendulum system.

We assume the equation of motion of the wire is expressed by that of a dangling string. By balancing the horizontal component of forces on an infinitely small element $z \sim (z+dz)$, the following equation is obtained as

$$(\frac{M}{\rho} + z)\frac{\partial^2\eta}{\partial z^2} + \frac{\partial\eta}{\partial z} - \frac{1}{g}\frac{\partial^2\eta}{\partial t^2} = 0 \quad (4)$$

where η is the lateral deflection of wire, z is the coordinate measured from the lowest end, ρ is the mass of string per unit length and M is the mass of load. Appling the finite difference method to the above equation using the following approximations,

$$\frac{\partial^2\eta}{\partial z^2} \simeq \frac{\eta_{i+1} - 2\eta_i + \eta_{i-1}}{\Delta z^2}\ ,\ \frac{\partial\eta}{\partial z} = \frac{\eta_i - \eta_{i-1}}{\Delta z}\ ,\ z = i\Delta z$$

we obtain

$$\frac{M}{\rho\Delta z}(\eta_{i-1} - 2\eta_i + \eta_{i+1}) + (i-1)\eta_{i-1} - (2i-1)\eta_i + i\eta_{i+1} = \frac{\Delta z}{g}\ddot{\eta}_i \quad (5)$$

where η_i is the lateral deflection of i-th mesh point numbered from the lowest end of the wire and Δz is the finite difference mesh.

From Eq.(5) and the equation obtained by replacing i by i+1 in Eq.(5), we obtain the following equation of motion by substituting $\theta_i = (\eta_i - \eta_{i+1})/\Delta z$,

$$\frac{\Delta z}{g}\ddot{\theta}_i = \frac{M}{\rho\Delta z}(\theta_{i+1} - 2\theta_i + \theta_{i-1}) + (i-1)\theta_i - 2i\theta_i + (i+1)\theta_{i+1} \quad (6)$$

The above equation is the same as the equation of motion of a multiple simple-pendulum system obtained from Eq.(3) if we regard Δz as the length of the simple pendulum and M as the additional mass to the lowest pendulum. This means that we can simulate the dynamics of wire in the form of a system of simple pendulums of length Δz.

The influence of a wire on the total dynamics of the pendulum system is quite small as can be seen in the experimental results. The exact dynamical formulation for a wire is not so important in our study (M is much greater than $\rho\Delta z$). So, we will not try to develop a more accurate mathematical model of the wire in this paper.

In the following numerical simulation, we will treat the wire-and-load system as a non-homogenous multiple pendulum system consisting of the uppermost rigid pendulum and a large-DOF series of simple pendulums, among them the lowest having a mass equal to that of the load.

3. Control Strategy

The concept of our vibration control is to connect the system whose vibration should be suppressed to a virtually infinite system that can absorb vibration energy endlessly. In the previous paper, we have presented a control strategy in which the real pendulum system is suspended by the imaginary energy-absorption multiple pendulum system whose dynamics is simulated by on-line computation. Since we have to use a finite-DOF energy absorption system in practice, we introduced initialization methods for the energy absorption system. At the time of initialization, the deflections and velocities of all the imaginary pendulums other than the lowest are set to zero, and the deflection and velocity of the lowest are set to fit the present position and velocity of the support of the real system.

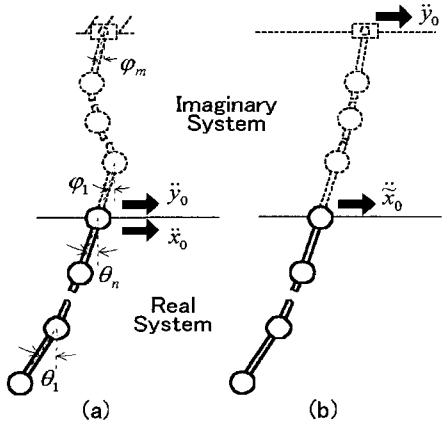

Fig. 2 Imaginary system for moving pendulum system
(a) Imaginary system for vibration control;
(b) Imaginary system for vibration and position control

In this paper, we treat vibration control of a suspended system that accepts a traveling command. The traveling command is given in term of the acceleration of the suspended system $\ddot{y}_c$ as a function of time. Two types of imaginary multiple-pendulum system are possible as shown in Fig. 2. One is the non-traveling imaginary system (NTIS, Fig. 2(a)) and the other the traveling imaginary system (TIS, Fig. 2(b)). The NTIS does not accept the traveling command $\ddot{y}_c$ and thus its algorithm is the same as that of the vibration control of the non-traveling system treated in the previous paper. The vibration control calculated using NTIS is added with the traveling command to produce position control of the support of the real system. The influence of the traveling is actually regarded as a disturbance appearing on the uppermost pendulum of the real system. With TIS, on the other hand, the support of the imaginary system is moved according to the traveling command $\ddot{y}_c$ and the movement is propagated through the imaginary system down to the real system. For both cases in Fig. 2, the value of $x_0 = \sum_{k=1}^{n} l_k\varphi_k$ is the distance between the horizontal positions of the support and of the lowest end of the imaginary system. The initialization is performed based on this value.

Through numerical simulations we have found the control performance using NTIS is better than that using TIS. It is considered that the initialization using TIS brings about a larger initial deflection and velocity to the lowest imaginary pendulum because the acceleration of the imaginary system due to $\ddot{y}_c$ produces a larger value of x_0. This causes the vibration energy flow back into the controlled real system. Therefore, we use NTIS in the following work.

Three types of initializing timing are investigated for NTIS as shown in Fig. 3. The cases (a) and (b) in Fig.3 are the same as those used in the previous paper, while (c) in Fig.3 is a new method presented in this paper. In the case (a), the PI method, initialization is made when $x_0 = 0 (= \sum_{k=1}^{n} l_k\varphi_k)$, and in the case (b), the VI method, initialization is made when $\dot{x}_0 = 0$. In the case (c), the VI method, initialization is made when $\dot{x}_0 = 0$ as in the case (b) but also has a position shift of the support of imaginary system. The vibration control performance in this case is better than in the cases (a) and (b), except that it may cause an error in the final support position of the real system.

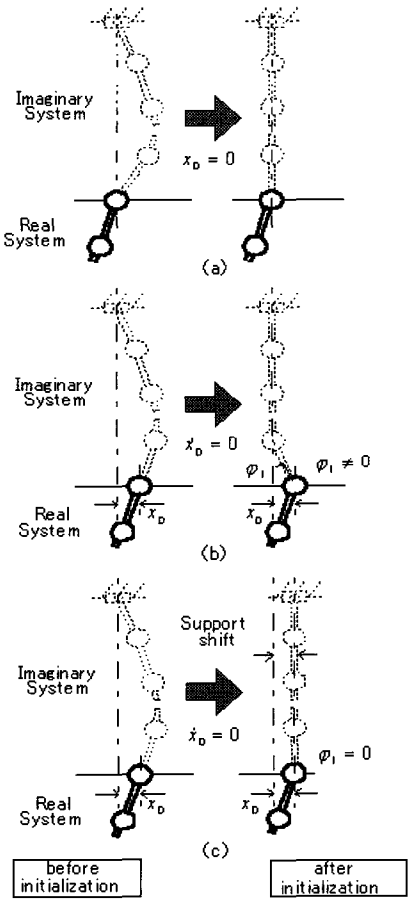

Fig. 3 Three types of initializing method
(a) PI method : initialization when $x_0 = 0$
(b) VI method : initialization when $\dot{x}_0 = 0$
(c) VI′ method : when $\dot{x}_0 = 0$ and support shift

It may be advantageous first to move the system near the destination with less vibration and then to control the final position accurately. It is an easy job for the control computer, given the present and target positions, to cancel the error of the final position.

When the real pendulum system is connected to the imaginary system, the acceleration of the lowest end of the imaginary system(Saigo et al., 1998) is represented as

$$\ddot{x}_0 = \frac{(i^2/l - h)\ddot{\theta} + g(\mu_0 + h/l)\theta - g(1 + \mu_0 + \mu)\varphi}{1 - h/l + \mu} \quad (7)$$

where θ is the angle of the uppermost rigid pendulum, φ is the angle of the lowest imaginary system pendulum, μ_0 is the ratio of the mass of the total real system to that of the uppermost rigid pendulum, μ is the ratio of the mass of an imaginary system pendulum to that of the uppermost rigid pendulum, and l, h and i^2 are the length, the distance between the supporting point and center of gravity, and the square of radius of gyration on the supporting point, of the uppermost rigid pendulum, respectively. As stated for the non-traveling case investigated in the previous paper, $\ddot{x}_0$ is used here also as the control of the movement of the support of the real pendulum system for vibration suppression. A homogenous multiple simple-pendulum system is used as the imaginary system in Eq.(7) for simplicity same as in the previous paper. A measured value of θ, the numerically approximated value of $\ddot{\theta}$ and the computed value of φ from the imaginary system give the vibration control $\ddot{x}_0$. Note that Eq.(7) includes no dimensional parameters of the suspended pendulums except those of the uppermost one. So, it can give vibration control for the multiple rigid-pendulum system as well as for the wire-and-load system with an uppermost rigid pendulum. In other words, the control does not depend on the length of the wire.

The parameter μ is introduced in Eq.(7) for the adjustment of the performance of the control system. For a large value of μ, the wave propagation in the imaginary system becomes slower and the control gain for the vibration suppression smaller. A smaller gain makes the control of the system more stable but less effective. In the experiment, we obtained the practical values for μ considering the system stability and the limitations of the actual DC servo motor system. Thus, the wave propagating characteristics in the imaginary system and the control performance of the vibration suppression can be designed by changing the values of μ. The parameter $\varkappa$, the ratio of the length of the imaginary system pendulum to that of the uppermost rigid pendulum, can also change the wave propagating characteristics in the imaginary system.

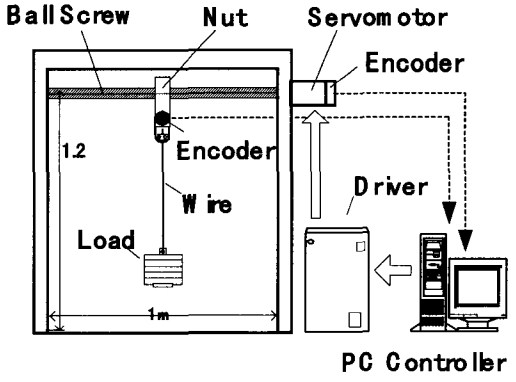

Fig. 4 Experimental apparatus for wire-load system

4. Experiment

4.1 Experimental apparatus

Fig. 4 shows a schematic diagram of the experimental apparatus. For multiple-pendulum system, it was demonstrated in the previous paper(Saigo et al., 1998), to which details are referred. The uppermost pendulum is connected to and supported by the nut of the ball-screw. The ball-screw is driven by a 350W DC servomotor to generate the horizontal movement of the support of pendulum. The DC servomotor is a velocity feedback type with an integrated tacho-generator. A rotary encoder is attached to the uppermost pendulum.

The multiple-pendulum system is made of three same-size aluminum plates connected serially by pins allowing free rotation. The width and thickness of each plate are 40 mm and 10 mm, respectively. The distance between the center axes of the connecting pins of each plate is 300 mm. The adjacent plates can be fixed rigidly with braces to form a pendulum system having less than three degrees of freedom.

The wire-and-load system is made up of a rigid pendulum, a wire and a load. The length, width and thickness of the rigid pendulum are 60 mm, 40 mm and 15 mm, respectively. The diameter of the wire is 1 mm. The length of the wire and the weight of the load can be changed.

The computation of the control is conducted by a DSP (TMS320C30) for the rigid-pendulum system and a personal computer with 200 MHz CPU for the wire-load system. The sampling period of A/D conversion is 0.1 ms for the rigid-pendulum system and 2 ms for the wire-and-load system. A 10-DOF system of simple pendulums has been used as the imaginary system.

The following system movement pattern is used as the traveling command in the experiments; the acceleration $\ddot{y}_c$ is 4.26 m/s^2 for the time period between 0 sec and 0.0352 sec, and -0.01883 m/s^2 between 0.0352 sec and 8 sec. Using this acceleration pattern, the pendulum system should travel the distance of 0.60 m in 8 seconds.

4.2 Experimental results of the multiple-pendulum system

Fig. 5 shows the effects of the different initializing methods, the PI and VI′ methods, for the 3-DOF traveling rigid-pendulum system with $\mu=3$. In Fig. 5, the curve rising to the right-hand side is the position of the support and the vibration waveform is the angle of the uppermost pendulum. We can confirm that our method is effective for a traveling pendulum system as well as for a non-traveling system. Fig. 6 shows the control performance of the PI method and the VI′ method on the 1-DOF pendulum system (three pendulums are connected rigidly). Both initializing methods have excellent vibration suppressing effects. Similarly, control performance on the nonhomogeneous 2-DOF pendulum system (the lowest and the middle pendulums are connected rigidly) is well confirmed, which is not presented here.

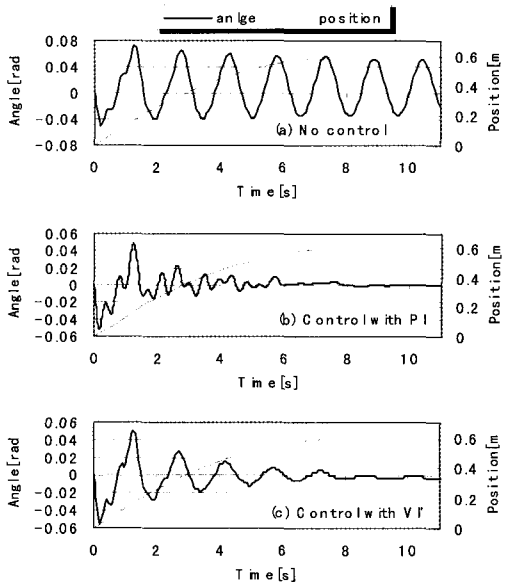

Fig. 5 Experimental results of 3-DOF pendulum system ($\mu=3$, $\varkappa=1$);
(a)No control,
(b)Control with PI method,
(c)Control with VI′ method

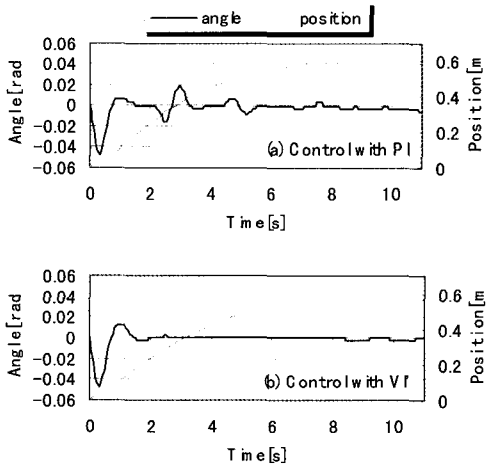

Fig. 6 Experimental results of 1-DOF pendulum system ($\mu=1$, $\varkappa=1$);
(a) Control with PI method,
(b) Control with VI′ method

4.3 Experimental results of the wire-and-load system

Fig. 7 shows the effects of the different initializing methods, the PI and VI′ methods, for the traveling wire-and-load system with the wire length l=0.5 m, the load weight w=12.3 N and $\mu=3$. In Fig. 7, the curve rising to the right-hand side is the position of the support and the vibration waveform is the angle of the uppermost pendulum. We can see that the VI′ method has quite an excellent damping performance (Fig. 7(c)). The PI method is accurate in positioning the pendulum system at the traveling destination, but the vibration control performance is not so good. The performance of the VI method is not so good, which is not shown here. The vibration waveform shown in Fig. 7(c) resembles well that of the 1-DOF rigid pendulum shown in Fig. 6(b). This means the dynamic characteristics of the experimental wire-and-load system is similar to that of the 1-DOF rigid-pendulum system and the vibration of the wire is practically negligible.

In order to understand the characteristics of the initializing methods obtained in the experiments, several numerical simulations have been conducted. Fig. 8 shows the simulation result for the wire-load system corresponding to Fig. 7(b) and 7(c). In the simulation, dry friction is assumed at each connecting pin of the pendulum to represent the wire. The ratio of the mass of the wire to that of the uppermost pendulum is assumed to be 0.0001.

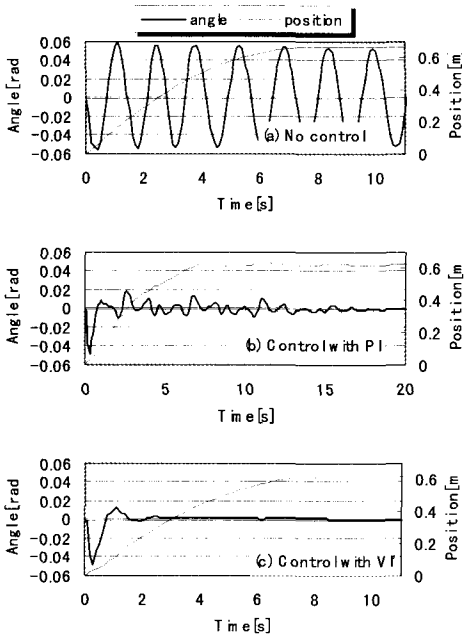

Fig. 7 Experimental results of wire-load system ($l=0.5m$, $w=12.3N$, $\mu=3$, $x=10$); (a) No control, (b) Control with PI method, (c) Control with VI′ method

Small wire vibrations occur at the starting period in the simulation results, which are not observed in the experiments. In Fig. 8 we show the waveform of the swing angle of the load in stead of that of the uppermost pendulum because the latter is affected by the small wire vibration. There is little difference between the results in Fig. 7 and Fig. 8. From these figures, we can confirm that the experiments have been performed successfully and that the angle of the uppermost rigid pendulum is virtually equal to the swing angle of the load.

As is easily understood, the vibration of the load would propagate up to the uppermost rigid pendulum. So, our wave-absorption system, which attends the uppermost rigid pendulum, is eventually effective in suppressing the vibration of the load. The VI′ method shows best vibration suppression among the three initializing methods. The PI and VI methods have inferior vibration control performances, especially for a small value of μ. Therefore, it is suitable to use a relatively large value of μ depressing the vibration control performance for the PI or VI methods.

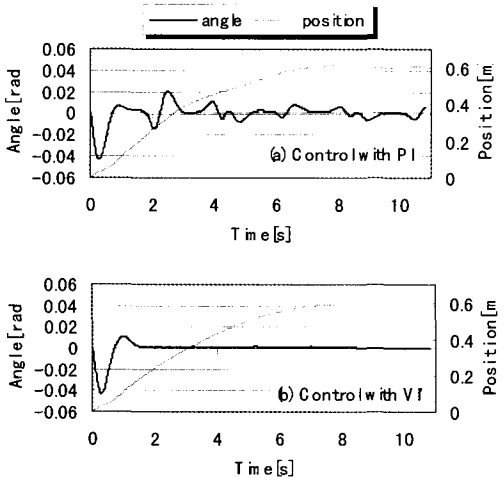

Fig. 8 Numerical results of wire-load system ($l=0.5m$, $w=12.3N$, $\mu=3$, $x=10$); (a) Control with PI method, (b) Control with VI′ method

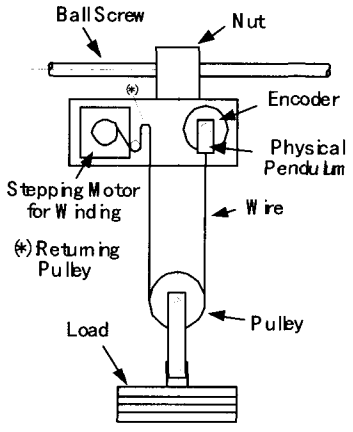

Fig. 9 Model crane system

4.4 Experimental results of model crane system

The wire-and-load system is extended to a model crane system that has a motor system to roll up and down the suspended mass like a real crane. Fig. 9 shows the experimental model of a crane, which has a load suspended by a wire and a pulley. One end of the wire is fixed to the motor shaft for winding and the other end is fixed to a small rigid pendulum that is attached to the nut of the ball-screw with free rotation. The distance between the axis of the rigid pendulum and the wire return on the returning pulley is equal to the diameter of the pulley. Then, the angle of the rigid pendulum is practically equal to the swing angle of the load independent of its height when the small vibrations of the wire can be ignored. This means the stationary direction of the pendulum is always vertical and the vibration suppression strategy for the wire-and-load system is applied directly by monitoring one half of the load suspension system. Our experiment has shown that it is possible to neglect the small wire vibration in the wire-and-load system as well as in most practical crane systems. The velocity pattern used of winding-up and rewinding-down is 0.1 m/s and -0.1 m/s, respectively. The load moves between the vertical positions of 0.9 m and 0.3 m during the time period between 0 sec and 6 sec.

Fig. 10 shows the experimental results for the case of winding up the load; (a) is the case where no vibration control is used, (b) is the case with wave control in the PI method, and (c) is the case with wave control in the VI′ method. Fig. 11 shows the cases of rewinding down the load with controls similar to those in Fig. 10. The system movement pattern is the same as in the case for the wire-and-load system. In Fig. 10, we can see the amplitude of the vibration in winding-up without control becomes larger as the wire length becomes shorter, due to the instability in winding-up of a suspended load. The contrast in these figures demonstrates the effectiveness of the stabilization using the wave-absorption control. In addition, the wave control method presented has shown an excellent control performance regardless of the wire length. Fig. 10(b) and Fig. 11(b) with the PI method for a large value of μ show relatively good results in the final state of the load, that is, accurate final position and small vibration. Thus, we can use the PI method to position the system accurately at the target position if its vibration suppression performance is acceptable. Even if the VI′ method is used, the final position errors are not very significant. Fig. 10 and Fig. 11 have shown our wave absorption method is useful for the actual crane system.

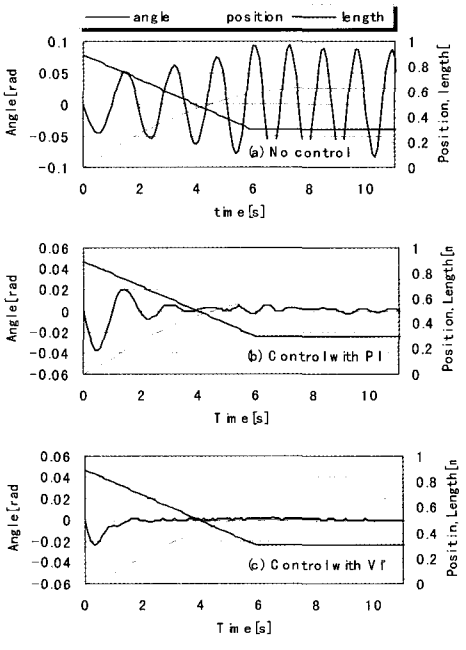

Fig. 10 Experimental results of crane system for load-raising (total weight = 17.6N);
(a) No control,
(b) Control with PI method ($\mu=10, x=10$),
(c) with VI′ method ($\mu=1, x=10$)

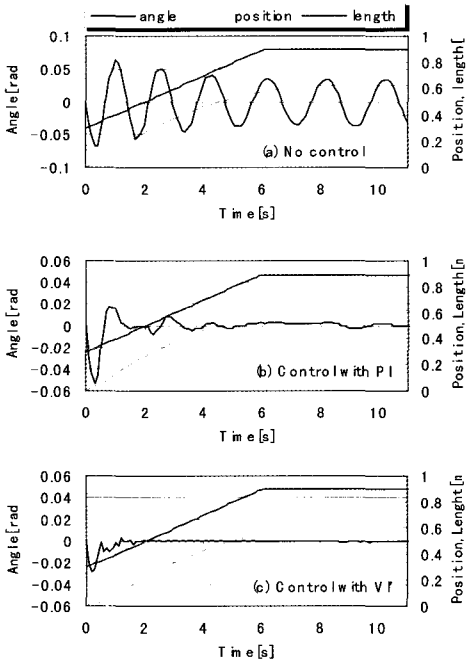

Fig. 11 Experimental results of crane system for load lowering (total weight = 17.6N);
(a) No control,
(b) Control with PI method ($\mu=10, x=10$),
(c) Control with VI′ method ($\mu=1, x=10$)

5. Conclusions

This paper proposes a wave control method using a non-traveling imaginary multiple-pendulum system applied to vibration control of the traveling suspended system. We have shown that the method presented, using little information about the suspended system states, is quite effective for a traveling suspended system whose dynamics are changeable during operation. The initializing methods with and without shifting the support of the imaginary system have their respective merits for the application. The former realizes accurate final positioning while the latter realizes excellent vibration suppression. Combination of methods can produce excellent overall performances. This control method can readily be applied to real crane systems that have a moving pulley and parallel wiring.

References

Fujii, H. and Ohtsuka, T. (1992). "Experiment of a Noncollocated Controller for Wave Cancellation", AIAA J. Guidance, Control and Dynamics, Vol 15-3, pp 741-745.

Mace, B.R. (1984). "Wave Reflection and Transmission in Beams", J. Sound & Vibration, Vol 97, pp 237-246.

Miller, D.W. and von Flotow, A.H. (1989). "A Travelling Wave Approach to Power Flow in Structural networks", J. Sound & Vibration, Vol 128, pp 145-162.

O'Connor, W. and Lang, D. (1998). "Position Control of Flexible Robot Arms Using Mechanical Waves", ASME J. Dynamic Systems, Measurement and Control, Vol 120, pp 334-339.

Saigo, M., Tanaka, N. and Tani, K. (1998). "An Approach to Vibration Control of Multiple-Pendulum System by Wave Absorption", ASME J. Vibration and Acoustics, Vol 120, pp 524-533.

Tanaka, N. and Kikushima, Y. (1992). "Active Wave Control of a Flexible Beam", JSME International Journal, Vol 35-1, pp 236-244.

Utsumi, M. (1999). "Analytical Implementation of Wave-Absorbing Control for Flexible Beams Using Synchronization Condition", ASME J. Vibration and Acoustics, Vol 121, pp 468-475.

Vaughan, D.R. (1968). "Application of Distributed Parameter Concepts to Dynamic Analysis and Control of Bending Vibrations", ASME J. Basic Engineering, Vol 90, pp 157-166.

Von Flotow, A.H. (1986a). "Traveling Wave Control for Large Spacecraft Structures", AIAA J. Guidance, Control and Dynamics, Vol 9, pp 462-468.

Von Flotow, A.H. (1986b). "Disturbance Propagation in Structural Networks", J. Sound & Vibration, Vol 106, pp 433-450.

2002년 12월 6일 원고 접수
2003년 1월 17일 최종 수정본 채택